MESO-SCALE MODELING OF WOVEN COMPOSITES: FROM THE PREFORMING OF THE FABRIC TO MECHANICAL PROPERTIES

G. Grail[1*], M. Hirsekorn[1], G. Hivet[2], R. Hambli[2]

[1] *ONERA, DMSC/MSC, 29 Avenue de la division Leclerc, 92322 Châtillon, France.*
[2]*Institut PRISME, 8 rue Léonard de Vinci, 45072 Orléans cedex 2.*
**gael.grail@onera.fr*

Keywords: woven composites, finite element meshing, meso-scale modeling

Abstract
A new approach to model composites with woven fiber reinforcements at the meso-scale is presented. It takes into account the yarn deformation occurring during preforming in the manufacturing process. It is based upon a new method to generate finite element meshes of the representative unit cells of woven composites, ensuring full contact between yarns, mesh conformity at the interfaces, and smooth, continuous yarn surfaces. The influence of the reinforcement compaction on the in-plane stiffness is studied. The model shows good agreement with experiments, and reveals that it is crucial to vary the yarn properties locally according to the yarn cross section. The method is highly flexible and the generated meshes well suited for the use in non-linear analysis and damage modeling.

1 Introduction

Woven composites are more and more used in the aeronautical industry because they present a good density/performance ratio and a high flexibility of the reinforcement allowing for optimization of the structural performances. They are fabricated by interlacing in crossed direction (0°/90°) two sets of fiber tows (warp and weft) in the case of 2D woven architectures. A third set (binder tows) is inserted in the out-of-plane direction in 3D woven architectures. Then, the dry fabric is draped in a mold, the resin is injected and finally both are cured to consolidate the material. This manufacturing process allows for a high adaptability which reduces labor and production costs compared to traditional laminated composites [1]. Moreover, the reinforcement composed of interlaced yarns in multiple directions offer, compared to composite laminates, better out-of-plane stiffness, strength, and toughness [2,3]. Depending on the structural needs, the optimum weave pattern may be very different, and has to be chosen among a quasi-infinite number of possibilities [4-7]. The potential of this kind of materials is very attractive, but in order to design woven composite structures that are really competitive compared to metals, it is necessary not only to optimize the constituents and their interaction between each other, but also the entire manufacturing process, in which each step has a strong influence on the structural properties of the composite [8-11]. For this reason, a link is needed between materials/manufacturing process parameters and structural performances of a woven composite part. In this contribution, we focus on the link between the fabric preforming step of the manufacturing process and the mechanical properties of the composite. Numerous models for the mechanical performances of woven composites have been developed by different research groups. A review of various models is given, e.g., by

Onal and Adanur [12] for 2D reinforcements, or by Ansar et al. [13] for 3D reinforcements. Analytical approaches give good predictions of the elastic homogenized properties of a Representative Unit Cell (RUC) of woven composites at the macro-scale, and have the advantage of low computational costs. Nevertheless, the capability to predict local stress and strain concentrations is limited. Therefore, FE models are needed in order to study nonlinear aspects, such as damage mechanisms [14]. Because of the strong is the influence of the fiber architecture on the material properties [4,5,7,14], the FE models have to represent the weave pattern as accurate as possible. This last point presents some difficulties and limits the applicability of this numerical approach [14]. Indeed, while numerous geometrical models of idealized weave pattern exist [15-18], meshing complex geometries of arbitrary woven architectures in a robust and automatic process remains a real challenge, and is beyond the capability of state-of-the-art automeshing programs [19,20]. To overcome these difficulties, several solutions have been proposed: the most common is imposing a small minimum distance between yarns in contact areas [15,17,21], which allows the creation of the matrix volume by simple boolean operations between a box and the yarns, available in most automeshing programs. The main drawbacks are that the mesh size in these spaces has to be very fine in order to avoid elements of poor quality, and that the matrix volume in the mesh is greater than in the real composite. Voxel elements offer an attractive alternative, but computational cost are high because the elements need to be very small, and local stress-strain concentrations at the interfaces of crimped yarns are not accurately predicted [19,20,22]. To the authors' knowledge, no general automatic and direct FE meshing method is currently available, which takes into account the reinforcement deformation after preforming and respects the continuity of the interface shapes.

A new method to generate FE meshes of woven composite RUCs with variable tow cross-section and full contact between yarns is proposed in Section 2. The objective is to link the deformation created by the preforming of the woven reinforcement to the mechanical properties of the composite. An unbalanced 4-ply plain weave E-Glass-epoxy laminate is modeled using a multi-scale approach (Section 3). The influence of preforming on in-plane homogenized elastic constants and on the local stress and strain distribution is analyzed in Section 4.

2 Mesh construction of a woven composite RUC with variable tow cross-sections

2.1 Parametric representation of yarn surfaces

The first step is to develop a general, robust and automatic geometry post-processing procedure that transforms the yarn geometries into a simple output format allowing their reconstruction by any kind of unstructured meshing tool. The entire procedure described below has been coded in MATLAB.

A yarn surface is generally represented by the yarn path and the cross-section. The yarn path is a one dimensional line following the yarn center in a three dimensional space. It can be described by a number of points, called master nodes, between which the line is interpolated. The cross-section is defined as the 2D shape of the yarn when cut by a plane perpendicular to the yarn path tangent. In general, it varies along the yarn path. We represent the yarn surfaces $P(u,v)$ using the parametric representation described by Sherburn [16], where u is the coordinate following the yarn path, while v follows the cross-section boundary. When this 2D parametric space is sampled, the yarn surface can be described by three matrices X, Y, Z, such that the position of each point P_{ij} on the yarn surface is given by:

$$P(u_i, v_j) = X(i,j)\,\boldsymbol{x} + Y(i,j)\,\boldsymbol{y} + Z(i,j)\,\boldsymbol{z}, \text{ with } 0 \le i < i_{max},\ 0 \le j < j_{max} \qquad (1)$$

If we ensure that each point is connected to its neighbors through the indexing of *X*, *Y* and *Z*, each yarn becomes a 3D grid whose denseness is controlled by the number of sample points i_{max} and j_{max}. Eq. (1) shows that the yarns grids can be decomposed into two types of lines (see Figure 1): j_{max} Yarn Lines $(YL_k)_{0\le k<j\max}$ and i_{max} Yarn Sections $(YS_k)_{0\le k<i\max}$. The Yarn Lines contain each i_{max} points $(P_{ik})_{0\le i<i\max}$, describing the yarn surface evolution along the yarn path direction. The Yarn Sections contain each j_{max} points $(P_{kj})_{0\le k<j\max}$, describing the yarn cross-section evolution along the yarn path. One line set for each yarn is sufficient to reconstruct the entire surface grid by interpolation and sample operations. This representation is thus very flexible: it is easily possible to build a yarn surface grid from a deformed hexahedral mesh or from a series of cross-sections along the yarn path, obtained from geometrical models or micro-tomography [15-17].

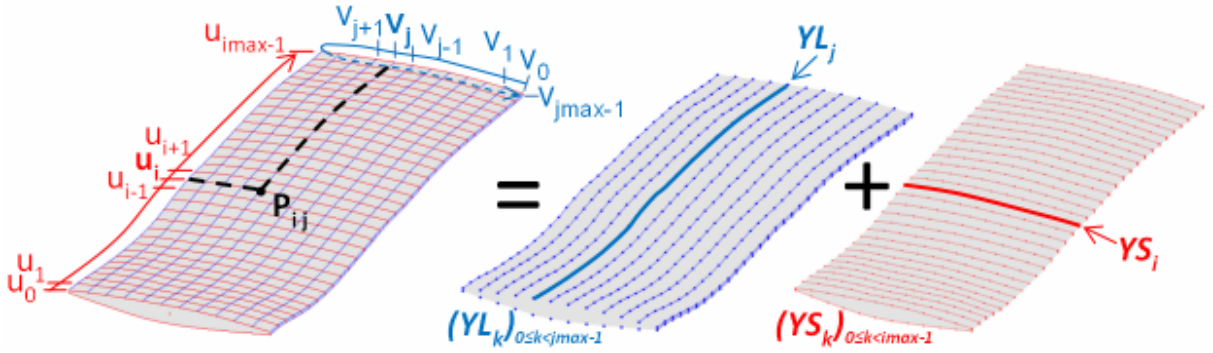

Figure 1. Parametric yarn representation

2.2 Conformity of yarns in contact areas

The meshes of two yarns are considered as conform if three conditions are met in the contact areas: (C1) they are sampled by the same number of nodes, which are (C2) at the same position, and (C3) have the same connectivity between them. In the geometrical model, the contact area must thus be represented by a unique topological entity which is common to both yarns. To the authors' knowledge, this is currently beyond the capability of state-of-the-art geometrical models when the yarn geometries are complex, especially when yarn deformation due to performing is taken into account.

The grid representation of the yarn surfaces described above, allows to generate a contact zone description meeting all three conditions by means of the two step procedure illustrated in Figure 2. The input parameters are the yarn grids and only one distance tolerance parameter *tol*.

Step 1 – Detection of contact areas (Figure 2a): The contact area between two yarns α_1 and α_2 is mapped by all points at the intersection of every line of $YL^{\alpha 1}$ with every line of $YL^{\alpha 2}$ if the yarn paths cross each other, or otherwise with every section of $YS^{\alpha 2}$. Two lines are considered to intersect if their minimum distance is below *tol*, and the intersection point is located at the center between the closest points on the lines.

Step 2 – Yarn grid reconstruction (Figure 2b and c): Once the contact points between every pair of lines have been detected, each line of YL^{α} or each section of YS^{α} of every yarn is separately rebuilt following two rules: (R1) a point cannot be inserted between two colored points of the same contact area, and (R2) every line or section belonging to the same yarn must contain the same number of points. Hence, (R1) ensures (C1) and (C2), while (R2) ensures a yarn representation through a parametric surface as described in Eq. (1). Figure 2b and c show the contact points, colored corresponding to the identification index α of the yarn in contact. After this procedure each yarn is still described by three matrices *X*, *Y*, *Z*, as in Eq.

(1). A fourth matrix *I* contains the identification indices of the contact areas: *I(i,j)* is the index at the point *Pij*. It is equal to 0 if *Pij* is not a contact point.

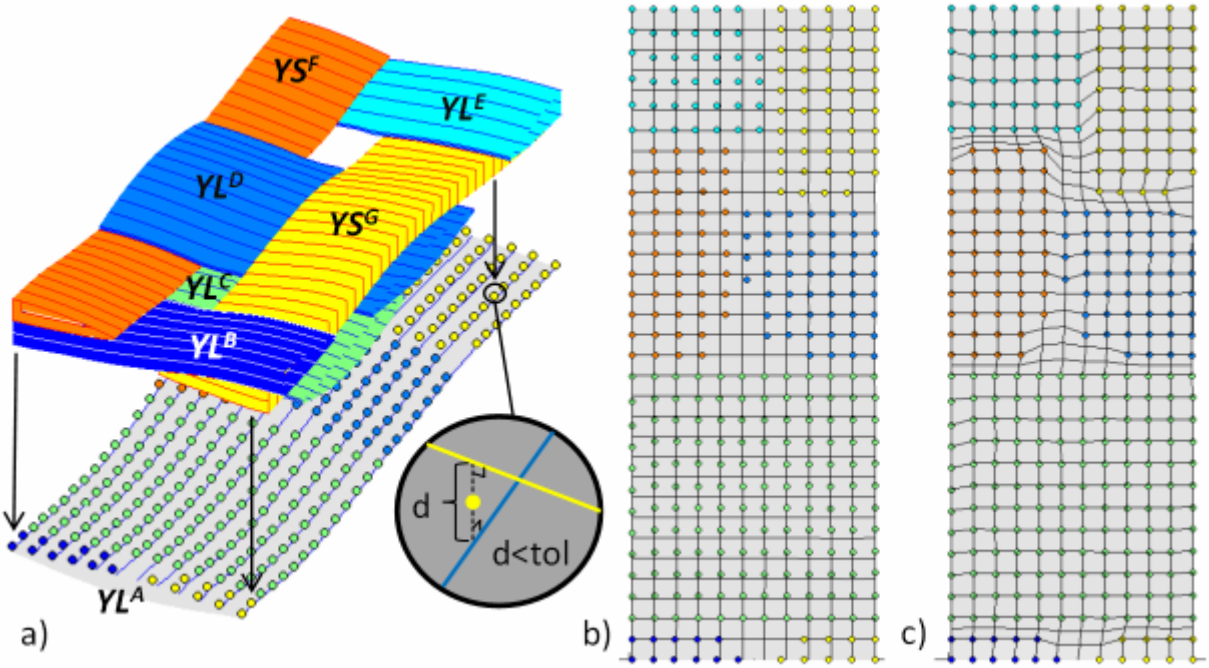

Figure 2. a) Contact detection between a yarn A and six other yarns [B-G] ; b) top view of yarn A with intersection points with yarns [B-G] ; c) top view of yarn A after grid reconstruction

2.3 Generation of a periodic unstructured FE mesh

Using the four matrices *X*, *Y*, *Z* and *I* for each yarn of the woven reinforcement, every node composing the yarn surface mapping can be constructed. Their respective position in the sampled 2D space given by the indices i and j (Eq. (1)), gives the connectivity to their neighbors, allowing the creation of all edges and faces needed to generate a mesh. As P_{ij}, P_{i+1j}, P_{i+1j+1} and P_{ij+1} are not coplanar, it is not possible to represent the surface by squares, but, triangle faces are allowed. Therefore, we have chosen to work with tetrahedral meshes. With the information given by the *I* matrix, the node connectivity is chosen such that the generated triangles have the best aspect ratio and respect the boundary of every contact area. Once each yarn mesh has been separately created, they can be fused as conformity at the contact areas has been ensured. Finally, the external faces of the composite RUC have to be built. Knowing position and connectivity of all reinforcement nodes, each boundary of each in-plane external face can be drawn, allowing for meshing the entire composite skin. A thin layer of matrix is inserted at the top and bottom side of the RUC, as our procedure does not create boundaries of out-of-plane external faces yet. If needed, this surface mesh can be improved by any auto-remeshing program. The mesh periodicity is ensured using the method proposed by Jean [23]. Finally, the volume mesh is then created by filling the interior of the closed surfaces of the surface mesh with tetrahedrons.

3 Multi-scale modeling of a preformed woven composite

3.1 Modeling the woven reinforcement compaction

The idealized meso-scale geometry of 4 layers of an unbalanced plain E-glass weave has been generated using the Hivet and Boisse model [18], with the parameters summarized in Table 2This geometry is meshed with hexahedral elements using the commercial software Abaqus (Figure 3a). 2D periodic boundary conditions are applied as described in [24], and a FE

calculation of fabric compaction is carried out. Parametric representations of the deformed yarns are obtained from the resulting deformed hexahedral mesh.

3.2 Construction of the RUC mesh for FE calculation with periodic boundary conditions

The deformed yarn geometries are post-processed using the procedure described in Section 2. The commercial automeshing tools Distene (http://www.distene.com/en/build/offer.html) are used to improve the surface mesh quality and to generate a volume mesh of quadratic tetrahedrons of the entire RUC (Figure 3b). Kinematic relations are applied between in-plane opposite nodes, in order to take into account the periodic nature of the woven reinforcement.

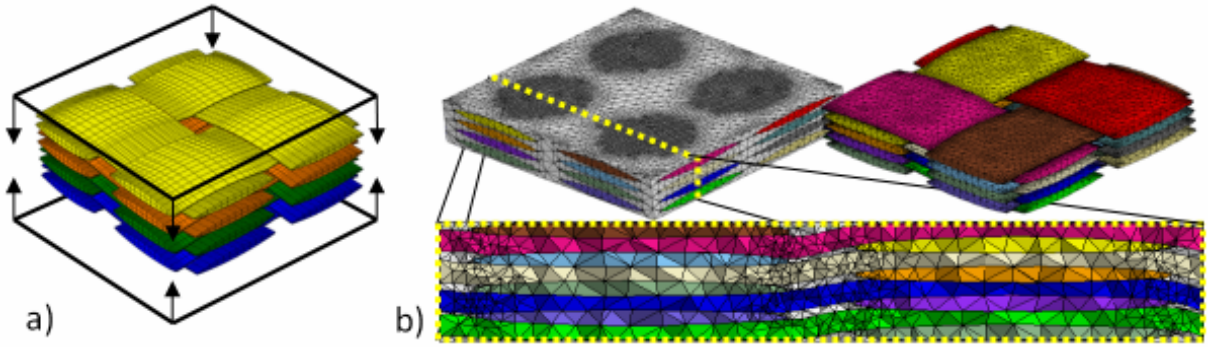

Figure 3. a) Mesh of 4 plies of plain weave reinforcement before compaction (total thickness: 2.906mm); b) Mesh of the composite with a compacted reinforcement (total thickness of the reinforcement: 1.691mm).

3.3 Micro-scale modeling and homogenized elastic properties of the yarns

Yarns are composed of locally almost parallel fibers embedded in matrix. At the meso-scale, they are represented by a homogeneous material, the properties of which are obtained by homogenization at the micro-scale. A FE calculation of a hexagonal micro-scale RUC is carried out using isotropic elastic linear behavior for matrix and fiber (material properties are given in Table 2). The fiber volume fraction in the yarns used in this calculation is adjusted such that the global fiber volume in the composite corresponds to that in the 4 layers of plain weave. Hence, the fiber volume fraction in yarns depends on the volume occupied by yarns in the RUC mesh obtained previously.

Thickness	0.72 mm
Yarn width	3.7 mm
Warp per cm	2.2
Weft per cm	2.
Weight per unit area	504 $g.m^{-2}$

Table 1. Properties of 1 ply of plain E-Glass weave

Fiber density	2.6 $g.cm^{-3}$
Fiber young modulus	72000 MPa
Fiber poisson ratio	0.3
Matrix young modulus	3200 MPa
Matrix poisson ratio	0.35

Table 2. Materials parameters

3.4 Yarn orientation

Since yarn crimp has a strong influence on the mechanical properties of the composite, it is important to use the correct local fiber orientation in the meso-scale RUC. The yarn direction in each integration point is obtained by orthogonal projection onto the central yarn path of the deformed reinforcement. This path is obtained by connecting the geometric centers of the sections from the parametric yarn representation.

3.5 Meso-scale modeling and homogenized in-plane elastic properties

The response of the composite RUC to tension in warp and weft direction and pure in-plane shear is calculated using the FE software Zset (http://www.zset-software.com/). Homogenized in-plane elastic constants are obtained from stress and strain average over the entire RUC.

4 Results and discussion

The homogenized in-plane elastic properties of the composite shown in Figure 3 have been calculated for different compactions using the material properties given in Table 2. The results are shown in Table 3 and compared to experimental data measured by means of tensile tests. Index 1 corresponds to the warp and index 2 to the weft direction. The thickness of the composite without compaction is 2.946 mm. For cases 1 to 5, the fiber volume in the yarns (measured experimentally) remains the same. Thus, the fiber volume fraction changes with the composite thickness. The calculated in-plane elastic constants increase linearly with the fiber volume fraction. For the highest compaction, the homogenized stiffness in the weft direction agrees well with the experimental results.

Case	Thickness (mm)	Compaction rate (%)	Fib. Vol. Frac. (%)	E_{11} (GPa)	E_{22} (GPa)	G_{12} (GPa)
1	2.946	0	27.64	14.1	13.9	4.39
2	2.277	22.7	33.99	16.5	16.3	4.84
3	1.925	34.7	40.01	18.7	18.6	5.58
4	1.731	41.2	44.72	20.7	20.6	6.06
5	1.651	44.0	46.88	22.3	21.7	6.61
exp	1.651 +- 0.02		46.88 +- 1		22.3 +- 2	

Table 3. Calculated and measured in-plane elastic constants

In the presented calculations, the in-plane stiffnesses are slightly underestimated, because the fiber volume fraction is assumed to be constant along the yarn path. However, due to compaction, the yarn cross section in the straight areas (where the yarns cross) is up to 10% smaller than in the crimped areas (see Figure 4). Therefore, with constant fiber volume fraction there are less fibers aligned with the load direction and more fibers in the crimped areas than in the real composite. This effect should be taken into account by varying the yarn properties locally according to the yarn cross section.

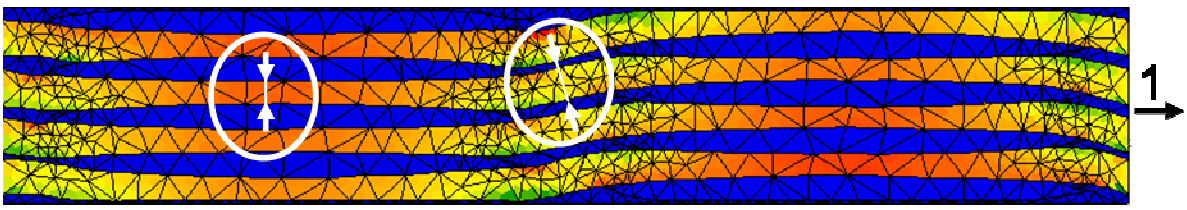

Figure 4. Local stresses in the direction 1, after a tensile test in the direction 1, for a compaction rate of 41.2 %

5 Conclusion

A new approach to model composite with woven reinforcement at the meso-scale has been presented. It takes into account yarn deformation occurring during preforming the reinforcement in the manufacturing process. A central part of the approach is a new method to

generate woven composite meshes. First, the reinforcement geometry, either obtained from geometrical models or from performing simulations, is converted into a simple parametric representation, which contains a description of all contact areas between yarns. This representation is then used to mesh the entire composite RUC with tetrahedral elements, ensuring mesh conformity at the interfaces, continuity of the yarn surfaces, and periodicity at boundaries. The entire method is automated, allowing for the generation of large number of different meshes needed for parametric studies. Using these meshes, the influence of the compaction on the in-plane homogenized elastic constants has been studied. Tensile and shear moduli increase linearly with the fiber volume fraction. Imposing a constant fiber volume fraction along the yarn path leads to a slight underestimation of the in-plane tensile moduli. This can be corrected by varying locally the yarn properties according to the yarn cross section.

The presented method offers a high flexibility and be easily applied to modeling nonlinear behavior and the effect of damage. Due to the conform meshing of the contact zones, it is no longer necessary to introduce artificial matrix layers between yarns in contact, which reduces significantly the computation time. Moreover, cohesive zone elements can be easily inserted at the yarn interfaces, and property degradation due to decohesion between yarns can thus be modeled. Finally, the continuity of the yarn surface avoids unphysical stress concentrations as would occur in voxel meshes, and allow thus for a more realistic estimation of the onset of damage at the meso-scale of composites with woven reinforcements.

References

[1] Mouritz A, Bannister M, Falzon P, Leong K. Review of applications for advanced three-dimensional fibre textile composites. *Composites: Part A,* **30,** pp. 1444-1461 (1999).

[2] Pearson JD, Zikry MA, Prabhugoud M, Peters K. Global-local assessment of low-velocity impact damage in woven composites. *Journal of Composite Materials,* **41,** pp. 2759-2783 (2007).

[3] El Hage C. Modélisation du comportement élastique endommageable de matériaux composites à renfort tridimensionnel. *PhD thesis of University of Bordeaux 1, France* (2006).

[4] Yanjun C, Guiqiong J, Bo W, Wei L. Elastic behavior analysis of 3D angle-interlock woven ceramic composites. *Acta Mechanica Solida Sinica,* **19,** pp. 152-159 (2006).

[5] Wu Z. Three-dimensional exact modeling of geometric and mechanical properties of woven composites. *Acta Mechanica Solida Sinica,* **22,** pp. 479-486 (2009).

[6] Lomov SV, Bogdanovich AE, Ivanov DS, Mungalov D, Karahan M, Verpoest I. A comparative study of tensile properties of non-crimp 3D orthogonal weave and multi-layer plain weave E-glass composites. Part 1: Materials, methods and principal results. *Composites: Part A,* **40,** pp. 1134-1143 (2009).

[7] Naik N K,.Ganesh V K. An analytical method for plain weave fabric composites. *Composites,* **26,** pp. 281-289 (1995).

[8] Gowayed Y,.Hwang JC. Thermal conductivity of composite materials made from plain weaves and 3-D weaves. *Composites Engineering,* **5,** pp. 1177-1186 (1995).

[9] Loix F, Badel P, Orgeas L, Geindreau C, Boisse P. Woven fabric permeability: From textile deformation to fluid flow mesoscale simulations. *Composites Science and Technology,* **68,** pp. 1624-1630 (2008).

[10] Laine B. Modélisation de la perméabilité des renforts fibreux utilisés dans la fabrication de pièces composites pour l'industrie aéronautique. *PhD thesis of ENSAM Paris, France* (2008).
[11] Daggumati S, De Baere I, Van Paepegem W, Degrieck J, Xu J, Lomov SV, Verpoest I. Local damage in a 5-harness satin weave composite under static tension: Part I – Experimental analysis. *Composites Science and Technology,* **70,** pp. 1926-1933 (2010).
[12] Onal L,.Adanur S. Modeling of elastic, thermal, and strength/failure analysis of two-dimensional woven composites - a review. *Applied Mechanics Reviews,* **60,** pp. 37-49 (2007).
[13] Ansar M, Xinwei W, Chouwei Z. Modeling strategies of 3D woven composites: A review. *Composite Structures,* **93,** pp. 1947-1963 (2011).
[14] Lomov SV, Perie G, Ivanov DS, Verpoest I, Marsal D. Modelling 3D fabrics and 3D-reinforced composites: challenges and solutions. *Textile Research Journal,* **81,** pp. 28-41 (2011).
[15] Couegnat G. Approche multiéchelle du comportement mécanique de matériaux composites à renfort tissé. *PhD thesis of University of Bordeaux 1, France* (2008).
[16] Sherburn M. Geometric and Mechanical Modelling of Textiles. *PhD thesis of University of Nottingham* (2007).
[17] Lomov SV, Ivanov DS, Verpoest I, Zako M, Kurashiki T, Nakai H, Hirosawa S. Meso-FE modelling of textile composites: Road map, data flow and algorithms. *Composites Science and Technology,* **67,** pp. 1870-1891 (2007).
[18] Hivet G,.Boisse P. Consistent 3D geometrical model of fabric elementary cell. Application to a meshing preprocessor for 3D finite element analysis. *Finite Elements in Analysis and Design,* **42,** pp. 25-49 (2005).
[19] Larve EV, Mollenhauer DH, Zhou EG, Breitzman T, Whitney TJ. Independent mesh method-based prediction of local and volume average fields in textile composites. *Composites: Part A,* **40,** pp. 1880-1890 (2009).
[20] Kim HK,.Swan CC. Voxel-Based Meshing and Unit-Cell Analysis of Textile Composite. *International Journal for Numerical Methods in Engineering,* **56,** pp. 977-1006 (2003).
[21] Stig F,.Hallström S. Spatial modelling of 3D-woven textiles. *Composite Structures,* **94,** pp. 1495-1 (2012).
[22] Potter E, Pinho ST, Robinson P, Iannucci L, McMillan AJ. Mesh generation and geometrical modelling of 3D woven composites with variable tow cross-sections. *Computational Materials Science,* **51,** pp. 103-111 (2012).
[23] Jean A. Etude d'un elastomere charge, de la nanostructure au macro-comportement. *PhD thesis of Mines ParisTech, France* (2009).
[24] Badel P, Vidal-Salle E, Boisse P. Computational determination of in-plane shear mechanical behaviour of textile composite reinforcements. *Computational Materials Science,* **40,** pp. 439-448 (2007).